Acta Biomaterialia 106 (2020) 114–123

Contents lists available at ScienceDirect

Acta Biomaterialia

journal homepage: www.elsevier.com/locate/actbio

Full length article

Bio-inspired hydrogel composed of hyaluronic acid and alginate as a potential bioink for 3D bioprinting of articular cartilage engineering constructs

Cristina Antich[a,b,c,d], Juan de Vicente[d,e], Gema Jiménez[a,b,c], Carlos Chocarro[a,b,d], Esmeralda Carrillo[a,b,c,d], Elvira Montañez[f], Patricia Gálvez-Martín[g,h,1,**], Juan Antonio Marchal[a,b,c,d,1,*]

[a] Biopathology and Regenerative Medicine Institute (IBIMER), Centre for Biomedical Research, University of Granada, Granada E-18100, Spain
[b] Instituto de Investigación Biosanitaria ibs.GRANADA, University Hospitals of Granada-University of Granada, 18100 Granada, Spain
[c] Department of Human Anatomy and Embryology, Faculty of Medicine, University of Granada, Granada E-18012, Spain
[d] Excellence Research Unit "Modeling Nature" (MNat), University of Granada, Spain
[e] Biocolloid and Fluid Physics Group, Department of Applied Physics, Faculty of Sciences, University of Granada, C/Fuentenueva s/n, 18071 - Granada, Spain
[f] Department of Orthopedic Surgery and Traumatology, Virgen de la Victoria University Hospital, 29010 Málaga, Spain
[g] Department of Pharmacy and Pharmaceutical Technology, School of Pharmacy, University of Granada, Granada E-18071, Spain
[h] Advanced Therapies Area, Bioibérica S.A.U., Barcelona E-08029, Spain

ARTICLE INFO

Article history:
Received 7 October 2019
Revised 9 January 2020
Accepted 29 January 2020
Available online 3 February 2020

Keywords:
Hyaluronic acid
Bioink
Bioprinting
Cartilage tissue engineering

ABSTRACT

Bioprinting is a promising tool to fabricate well-organized cell-laden constructs for repair and regeneration of articular cartilage. The selection of a suitable bioink, in terms of composition and mechanical properties, is crucial for the development of viable cartilage substitutes. In this study, we focused on the use of one of the main cartilage components, hyaluronic acid (HA), to design and formulate a new bioink for cartilage tissue 3D bioprinting. Major characteristics required for this application such as printability, biocompatibility, and biodegradability were analyzed. To produce cartilage constructs with optimal mechanical properties, HA-based bioink was co-printed with polylactic acid (PLA). HA-based bioink was found to improve cell functionality by an increase in the expression of chondrogenic gene markers and specific matrix deposition and, therefore, tissue formation. These results indicate that it is a promising bioink candidate for cartilage tissue engineering based in 3D bioprinting.

Statement of Significance

The recent appearance of 3D printing technology has enabled great advances in the treatment of osteochondral disorders by fabrication of cartilage tissue constructs that restore and/or regenerate damaged tissue. In this attempt, the selection of a suitable biomaterial, in terms of composition and mechanical properties, is crucial. In this study, we describe for first time the development of a bioink based on the main component of cartilage, HA, with suitable biological and mechanical properties, without involving toxic procedure, and its application in cartilage tissue bioprinting. Hybrid constructs prepared by co-printing this bioink and thermoplastic polymer PLA provided an optimal niche for chondrocyte growth and maintenance as well as mechanical properties necessary to support load forces exerted in native tissue. We highlight the translation potential of this HA-based bioink in the clinical arena.

* Corresponding author: Department of Human Anatomy and Embryology, Faculty of Medicine, University of Granada, Parque Tecnológico de la Salud, Av. de la Investigación, 11, 18016 Granada, Spain.
** Corresponding author: Advanced Therapies Area, Bioibérica S.A.U., Barcelona E-08029, Spain.
E-mail addresses: galmafarma@gmail.com (P. Gálvez-Martín), jmarchal@ugr.es (J.A. Marchal).
[1] These authors contributed equally to this work.

https://doi.org/10.1016/j.actbio.2020.01.046
1742-7061/

1. Introduction

Articular cartilage (AC) is a highly specialized connective tissue that due to its compositional and structural nature has a limited capacity for self-repairing, a condition that leads to degeneration upon injury. In this situation, clinical intervention is necessary. Recently, tissue engineering (TE) has emerged as an inter-disciplinary field to develop new therapeutic approaches for cartilage regeneration based on the generation of biological substitutes that restore, maintain, or improve damaged tissue function [1,2]. Generally, this is performed by culturing the cells in a 3D mesh or scaffold that provides a mechanically supportive microenvironment [3].

The introduction of three-dimensional (3D) bioprinting technology in TE has led a great progress as it allows to attain tissue analogue structures by controlled 3D deposition of living cells and supporting biomaterials in a spatial location [4]. To date, several dispensing techniques have been developed to mimic the anatomy of articular cartilage tissue. These include inkjet, laser-induced forward transfer (SLA), stereolithography, and Extrusion-based plotting (EBP), which is the most common and affordable bioprinting method [5]. Using this specific technique, researchers have reported the creation of cartilage-like constructs solely by the combination of different hydrogels [6–13], although the most suitable strategy has involved simultaneous deposition of thermoplastic polymers (e.g. polylactic acid, PLA), as structural materials capable of resisting mechanical forces, and hydrogels as cell carriers [14–16]. In this case, there are many biomaterial candidates that provide a suitable microphysical environment and excellent biocompatibility [10,17,18], but not all provide the physiological conditions of the living tissue to obtain functional engineered constructs.

Hyaluronic acid (HA) is a structurally simple, polymeric glycosaminoglycan (GAG) composed of repeating units of $\beta-1,4$-D-glucuronic acid-$\beta-1,3$-N-acetyl-Dglucosamine residues. It is a main component in the extracellular matrix (ECM) of AC, where it plays a critical role in maintaining cartilage homeostasis by the regulation of cell functions, including promotion of chondrogenic phenotype, and production and retention of matrix components [19]. Despite these bioactive properties and excellent biocompatibility that have made HA a fascinating biomaterial for cartilage tissue engineering, it lacks the physical properties required for its application in 3D extrusion-based bioprinting (EBB). Among these limitations, solutions of this material do not have enough viscosity to ensure stability in the reservoir for the time of the printing procedure, and therefore, homogeneous three-dimensional distribution of the cells. HA also lacks gelation abilities that are essential to maintain 3D structure after the printing process [20,21].

Several strategies based on modification of HA have allowed the development of HA formulations suitable for use as a bioink [22–26]. However, most of them have some issues that can limit their practical use. In this context, combination with natural gelling agents has gained considerable attention as they do not involve any toxic or complex process during preparation and gel formation [27–29]. In the present study, a new HA-based bioink was designed by including alginate, a biomaterial outstanding for its biocompatibility, mechanical properties and fast gelation kinetics [14,30,31] to 3D bioprint a hybrid construct for AC regeneration. Mechanical properties of the HA-based bioink and 3D hybrid construct were analyzed and the biological feasibility of the bioprinting construct was assessed by using primary human chondrocytes and testing cell viability, karyotyping, proliferation, and protein and gene expression.

2. Materials and methods

2.1. Isolation and culture of chondrocytes

Articular cartilage was obtained from the AC of osteoarthritic patients. Ethical approval for the study was obtained from the Ethics Committee of the Clinical University Hospital of Málaga, Spain. Informed patient consent was obtained for all samples used in this study. None of the patients had a history of inflammatory arthritis or crystal-induced arthritis. Human articular chondrocytes were isolated as previously described [32]. Briefly, cells were obtained from the femoral side by selecting the non-overload compartment: lateral condyle in varus knees and medial condyle in the valgus cases. Only cartilage that macroscopically appeared relatively normal was used for this study. Chondrocytes were grown in DMEM–high glucose (Sigma) supplemented with 10% fetal bovine serum (Gibco), 50 μg/μL of L-ascorbic acid 2-phosphate (Sigma), 40 μg/μL of L-proline (Sigma), 1% penicillin-streptomycin (Sigma) and 1% insulin-transferrin-selenium (Gibco) in a 25-cm^2 cell culture flask. Cells were incubated at 37 °C humidified atmosphere containing 5% CO_2 and expanded in a monolayer for 7–10 days before the experiment.

2.2. Quantitative real-time PCR (qPCR)

Total messenger RNA (mRNA) was isolated using TriReagent (Sigma) and reverse-transcribed into cDNA using the Reverse Transcription System kit (Promega). The quantitative real-time polymerase chain reaction (qRT-PCR) was conducted using a SYBR green master mix (Promega) according to the manufacturer's recommendations. Gene expression levels for aggrecan (ACAN), type II collagen (COL2A1), Sox-transcription factor 9 (SOX-9), type I collagen (COL1A1) and type X collagen (COL10A1) levels were normalized to those of the housekeeping gene glyceraldehyde 3-phosphate dehydrogenase (GADPH) and shown as fold change relative to the value of the control sample (alginate hybrid scaffold). The primer sequences are reported in previous work [32]. All the samples were done in triplicate for each gene.

2.3. Preparation of the HA-based bioinks

The bioink formulation consisted of an HA-based hydrogel capable of forming physically cross-linked gels in the presence of calcium. It was prepared by dissolving HA and alginate (A) in deionized water at concentrations of 1% (w/v) and 2% (w/v), respectively (Fig. 1A). This formulation was identified to have greater effectiveness in chondrogenesis assays, after testing a wide range of HA concentrations by gene expression (Figure S1). Moreover, this particular concentration is the most commonly used for clinical viscosupplementation. Finally, to obtain the final bioink, chondrocytes were suspended at the desired concentration (1×1010^6 cells/mL) in the solutions (Fig. 1B). Two other hydrogels consisting of A at 2% (w/v) and HA at 1% (w/v) respectively, were also prepared as a control.

2.4. Rheological tests of bioinks

All the rheological tests were carried out in a torsional rheometer MCR302 (Anton Paar, Austria) at 25 °C.

2.4.1. Steady shear and linear viscoelasticity of the hydrogels

The hydrogels were measured using cone-plate geometry (50 mm diameter and 1° angle). The shear viscosity was obtained

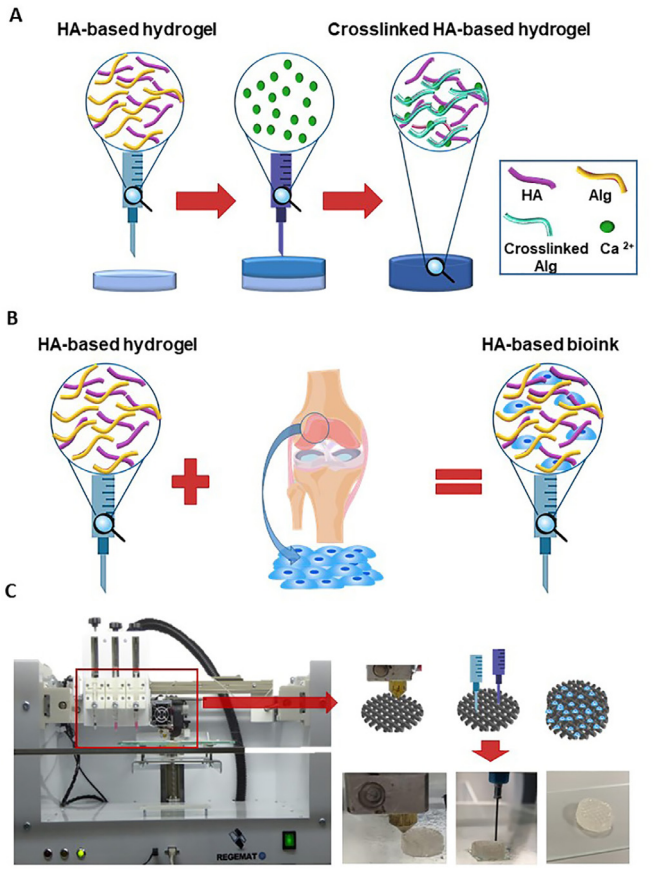

Fig. 1. (a) Hydrogel formulation. (b) Preparation of HA-based bioink (hydrogel). (c) Scheme of 3D bioprinting process of articular cartilage engineering.

in a three-step protocol. First, the hydrogel was pre-sheared at 1000 s^{-1} for 1 min. Then, it was allowed to rest (without a shear rate applied) for 1 min. Finally, the shear rate was logarithmically increased from 0.1 to 1000 s^{-1} (acquisition time of 5 s) for 5 min.

The viscoelastic properties were also investigated in dynamic oscillatory shear. We performed strain amplitude and frequency sweeps, again, in a three-step process. The first and second steps were similar to the ones for steady shear tests while the third one consisted of either increasing the strain amplitude from 10% to 1000% at a constant frequency of 1 Hz, or decreasing the excitation frequency from 100 to 0.1 Hz at a constant strain amplitude of 10%.

2.4.2. Dynamic oscillatory shear behavior of the crosslinked hydrogels

HA-based hydrogels were crosslinked using calcium (100 mM $CaCl_2$) in molds having disk-like shapes and then placed on top of the rheometer for testing. The mechanical properties were measured using a plate-plate geometry with 20 mm diameter and 5 mm gap. The viscoelastic properties were determined as follows. After the specimen was placed on top of the lower base of the rheometer, the rheometer head was displaced downwards at a constant velocity of 10 µm/s. Once the head registers a normal force that is larger than 0.5 N, the rheometer head stops and the normal force is kept constant at 0.5 N for 30 more seconds. Finally, the sample is subjected to an oscillatory shear of 0.1% strain amplitude and an excitation frequency of 1 Hz at a constant normal force of 0.5 N to quantify the viscoelastic properties.

2.4.3. Degradation rate of HA-based bioinks using linear viscoelasticity

HA-based bioinks were prepared, as previously described and then crosslinked to form a disk-like shape. The degradation rate of the bioinks was studied through the evolution of their viscoelastic moduli as a function of time over a month. We prepared as many identical samples as time points, keeping them under the same culture conditions up to the measurement time point. For the experiments, we followed the same rheological protocol as previously described.

2.5. Bioprinting of hybrid 3D scaffolds with HA-based bioinks

The design of the construct was based on the combination of the positive attributes of the PLA synthetic polymer that confers superior mechanical properties and natural biopolymers (HA and A), which provide a supportive native-like environment for cell encapsulation. It was fabricated using the REGEMAT V1 bioprinter as previously described [16]. Briefly, the bioprinting process involves a dual-step procedure: deposition of a thermoplastic polymer framework and injection of the bioink and $CaCl_2$ solution into that structure. First, PLA was deposited by head (at 200 °C) in a layer-by-layer manner to generate the framework that was previously designed using software REGEMAT 3D designer (porous cylinder-type structure, 10 × 10 mm; 600 µm pore size). After printing 4 layers, the HA-based bioink with chondrocytes loaded in a syringe (3 cc) was injected into the pores of PLA structure. Then, it was physically cross-linked by following with an injection of 100 mM $CaCl_2$, loaded into another syringe (Fig. 1C). This procedure was repeated until the scaffold was completely built. We bioprinted as many cell-laden scaffolds as were needed for following analytical studies. Finally, hybrid constructs were cultured in growth medium at 37 °C in 5% CO_2 atmosphere.

2.6. Mechanical testing of the scaffolds

The mechanical properties of the hybrid constructs were investigated using compression and shear tests. The test consisted of the following stages. First, a scaffold with cylindrical shape (20 mm diameter and 5 mm height) was placed onto the base of the rheometer. Then, the rheometer head was approached at a constant speed (10 µm/s) up to a normal force reading of 40 N. At that stage, the specimen was oscillatory sheared according to a strain amplitude of 0.00001% at a frequency of 1 Hz and a normal force of 40 N to determine the shear viscoelastic moduli and finally the upper plate was separated at a constant speed (10 µm/s). The compression and tension steps allowed to determine the compression modulus, while the shearing step allows us to determine the shearing modulus.

2.7. Cell viability

The Live/Dead assay (Thermo Fisher Scientific) was used to evaluate the viability of chondrocytes previous to and after the bioprinting process at 24 h, 1, 2, 3, and 4 weeks in culture. Briefly, cell-laden scaffolds were washed and stained with 4 µL of 2 µM calcine AM and 8 µL of 4 µM EthD-I in 4 mL of sterile phosphate-buffered saline (PBS), incubated in the dark for 30 min. After washing with PBS, the scaffolds were observed using a confocal microscope and imaged. Green fluorescence was visualized in live cells and red fluorescence in dead cells using two different filters. Images were analyzed with Image J software (v. 1.52i, USA). For each cell type, six regions were counted to obtain an average value of the percent of viable cells ($n = 3$).

2.8. Cell proliferation

The proliferation rate of chondrocytes encapsulated in 3D hybrid constructs were assessed by colorimetric alamar Blue (aB) assay (Thermo Fisher Scientific) at day 0 and 1, 2, 3 and 4 weeks after bioprinting. Cell-free 3D scaffolds were used as controls, and data was normalized to the appropriate control. Briefly, at each time point, scaffolds were incubated with 10 µL of aB solution per 100 µL of medium and incubated for 3 h. The fluorescence intensity was measured using a plate reader (Synergy HT, BIO-TEK) with excitation and emission wavelengths of 570 and 600 nm, respectively. The absorbance data was represented as fold increase to day 0. Experiments were performed in triplicate ($n = 3$).

2.9. Karyotype analysis

Karyotype analysis was performed before and after bioprinting process by G band techniques. To obtain chromosomal preparations, chondrocytes were treated with 0.8 mg/mL colchicine and incubated at 37 °C for 1.15 h. Then, cells were collected and digested into 0.05% trypsin, continued with a hypotonic treatment using 0.075 mol/L KCl and fixation in the mixture of methanol and glacial acetic acid. Mitosis metaphase spreads were stained with Giemsa dye and imaged under the optical microscope. Approximately 20 metaphases were analyzed under the microscope. The final result was described to account for the recommendations from the International System for Human Cytogenetic Nomenclature.

2.10. Biochemical assays

For GAG quantification, 3D hybrid constructs were digested in 1 mL of papain solution (125 mg/mL papain in 0.1 M sodium phosphate with 5 mM EDTA and 5 mM cysteine-HCl at pH 6.5) for 16 h at 60 °C. Then, they were centrifuged at 10,000 × *g* for 5 min. The supernatant was used for chemical assay, and the quantity of GAGs was measured by the dimethylmethyleneblue (DMB) colorimetric assay. The supernatant was mixed with DMB solution to bind GAGs. The content was calculated based on a standard curve of sulfate chondroitin from shark cartilage (Sigma) at 530 nm on a microplate spectrophotometer and normalized with cell-free laden scaffolds. The DNA content was determined by a Hoechst assay. The supernatant was reacted with the Hoechst dye for 30 min in the dark. The intensity of fluorescence was screened with a 96-well plate reader (excitation at 360 nm and emission at 460 nm). The content was calculated using thymus DNA for a standard curve (Sigma).

For type II collagen quantification, 3D hybrid constructs were digested by pepsin (1 mg/mL) in 0.5 N acetic acid for 48 h at 4 °C followed by adding 1 mg/mL pancreatic elastase solution at 4 °C for 24 h. Finally, the samples were neutralized with 1 M Tris base. The insoluble material was removed by centrifugation at 10,000 rpm at room temperature for 5 min, and the supernatant was collected for assay. The quantitative analysis was performed using a commercially available Type II collagen ELISA kit (Chondrex), according to manufacturer's instructions and measured on Microplate Spectrophotometer at 490 nm.

2.11. Statistical analysis

Statistical analysis was performed using SPSS software (version 17.0). Unpaired *t*-test was used for single comparison between groups. All results are shown as mean and standard deviations. A difference between the mean values for each group was considered statistically significant when the p value was less than 0.05.

3. Results and discussion

3.1. Effect of HA concentration

Previous to bioink formulation, we determined the optimal HA concentration for preservation and improvement of chondrogenic phenotype. It was analyzed by gene expression of chondrocytes embedded in hydrogels at different concentrations of HA after 14 days in culture. These concentrations were selected based on those reported in the literature [33–35]. As shown in Figure S1, the addition of HA to alginate hydrogel caused an overall increased expression of chondrogenic markers such as Collagen type II (COL2A1), Aggrecan (ACAN), and SOX9, especially in 1% HA. Significantly higher levels for all these genes were observed than those for the remaining conditions, although the levels were similar to 0.5% and 5% in the case of ACAN and SOX9, respectively. Moreover, there was a trend toward a reduction of dedifferentiation markers, such as fibrotic marker collagen type I (COL1A1) [36] and hypertrophic marker COL10A1 [37], in presence of HA. However, it was not statistically significant in comparison to alginate, whose expression was not detectable or very low for all conditions studied. . Altogether, these results indicated that 1% HA provided the most favorable environment to preserve and enhance the phenotype of chondrocytes.

3.2. Characterization of the bioink

The rheological properties of the bioink are crucial for an optimal performance in the extrusion process through the syringe. For this reason, both steady shear and dynamic oscillatory properties were investigated.

3.1.1. HA-based hydrogels

The viscosity versus shear rate curves for the three hydrogels based on A, HA and *A*+HA, are shown in Fig. 2A. As observed, A exhibits a constant shear viscosity as expected from a Newtonian material. However, HA alone or combined with A exhibits a shear thinning behavior (i.e. decrease of viscosity with shear rate) that is expected in view of the large molecular weight of the HA molecule. This result is in accordance with the literature where it was previously reported that HA was widely explored as a "building block" in various bioink formulations for cartilage bioprinting in CTE because of its viscoelastic and bioactive properties [38]. Even though the shear rates achieved in the extrusion process are expected to be larger than the maximum shear rates achieved in the rheometer (a rough estimation can be obtained from the flow rate and the diameter of the nozzle 250 µm), the viscosity level is expected to remain below 100 mPa. Therefore, the bioinks are expected to be easily extruded without significant effort [17,39].

The strain amplitude sweep tests for the three hydrogels investigated exhibit a linear viscous behavior ($G'' > G'$) in a wide range of strains for all hydrogels (Fig. 2B). These results are in agreement with viscosity data in Fig. 2A. The samples show purely dissipative solutions.

In Fig. 2C, we show frequency sweep results in the linear viscoelastic regime (i.e. low strain region in Fig. 2B) for the three hydrogels investigated. As expected, the data demonstrates that the hydrogels behave as viscous materials in a wide range of frequencies ($G'' > G'$). The slope of the G'' curve agrees well with the shear viscosity shown in Fig. 2A.

3.1.2. Crosslinked HA-based hydrogel

As stated in the Materials and Methods section, calcium solutions were used to crosslink the hydrogel. This particular gelation process is extraordinarily rapid and cannot be followed in situ within the rheometer. Once the cylinders were completely gelled

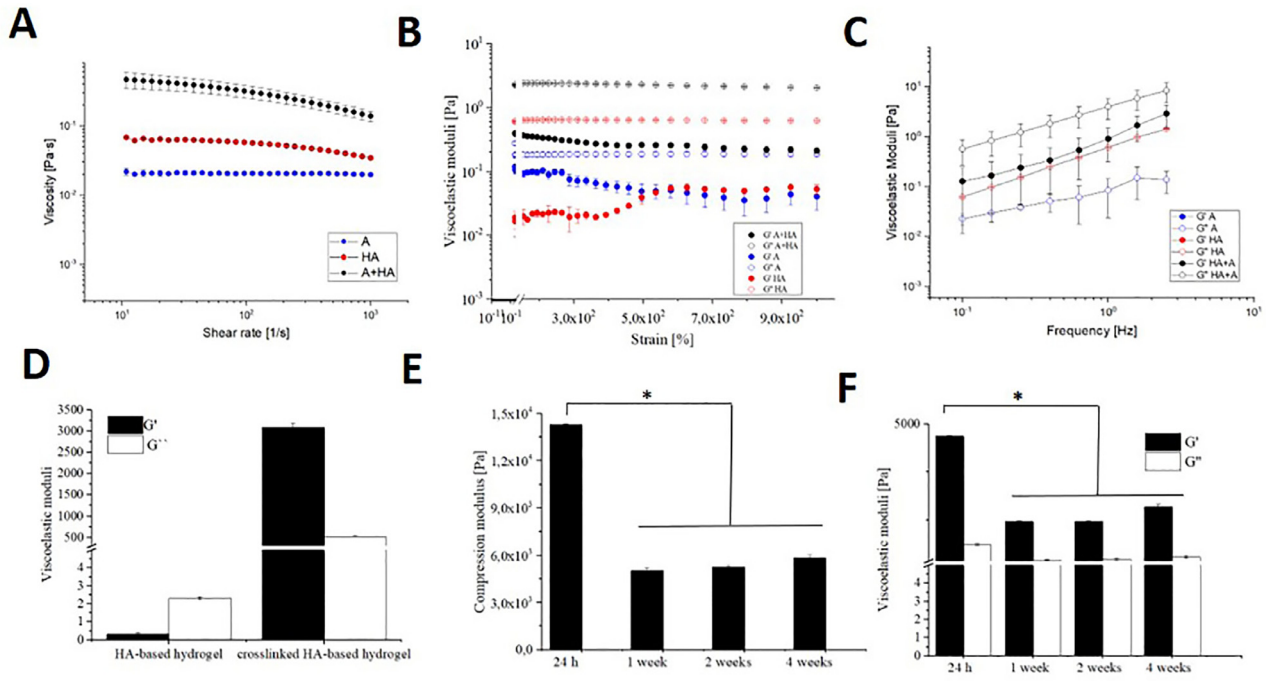

Fig. 2. Rheological characterization. (a) Viscosity curves of alginate, hyaluronic acid (HA) and A+HA hydrogels. (b) Strain amplitude sweeps in dynamic oscillatory shear of the three hydrogels. Frequency = 1 Hz. (c) Frequency sweep in dynamic oscillatory shear of the three hydrogels. Strain amplitude = 0.1%. (d) Viscoelastic moduli of HA-based hydrogels and crosslinked HA-based hydrogel (*A*+HA). Compression (e) and viscoelastic moduli (f) of the crosslinked HA-based hydrogel over 1 month in culture. The experiments were performed in triplicate. (mean ± SD, $n = 3$, Student's *t*-test, $^{*}p < 0.05$).

(after 1 h in the presence of $CaCl_2$), the specimens were loaded onto the rheometer and the tests initiated.

The viscoelastic moduli of the crosslinked HA-based hydrogel are shown in Fig. 2D together with those obtained from the solutions in the low strain amplitude region in strain amplitude sweeps (see Fig. 2B). As expected, the storage modulus G′ of the crosslinked HA-based hydrogel becomes larger than the loss modulus G″ and clearly above those measured in hydrogels. The storage modulus reaches a value of approximately 3 kPa. In accordance with Honghyun Park et al. [40], this value is sufficient for the gel to hold the cells in place, while still allowing them to proliferate and grow.

3.1.3. Crosslinked HA-based bioink degradation

The long-term stability of the crosslinked HA-based bioink was investigated through changes in material rheological behavior with time. Compression and viscoelastic moduli were recorded over a culture period of 4 weeks. Both moduli exhibited similar trends. As shown in Fig. 2E and F, there was a significant decrease in both moduli after 1 week, probably due to the gel dissociation by ionic exchange of the Ca^{+2} with Na^{+} in the culture medium and the degradation of HA by hyaluronidases secreted from cells [41–43], but then they were kept unchanged until the end of the test. A very slight increase with time was observed that could be correlated to new tissue synthesis.

3.2. Mechanical properties of the bioprinted scaffolds

The mechanical properties of the bioprinted scaffolds are crucial for clinical applications. Hence, we analyzed the compression moduli for the three scaffolds investigated (Fig. 3A). The range between 1.5 and 3 MPa and HA incorporation increased the modulus as compared to A alone-PLA scaffolds and even more than PLA-alone construct. This enhancement in mechanical properties could be related to the large colloid osmotic pressure and viscoelasticity properties of HA that provides load bearing capability. After 4 weeks in culture, their modulus increased, but there was no significant difference between them. In Fig. 3B, we show the shear (viscoelastic) moduli of the construct. The loss moduli are negligible while the storage moduli are in the range of MPa. Similar to compression moduli, their values increased after culture period, maintaining the difference between them. These values, for compression and shear moduli, are comparable to those of healthy human articular cartilage [44,45]. Moreover, they are in agreement with results from other 3D constructs that have been used for CTE [26,46–49].

3.3. Cell viability of the bioprinted scaffolds

The main goal of fabrication using 3D bioprinting technology is to achieve high cell viability in constructs. During this process, chondrocytes are exposed to shear stress induced by nozzle and high melting temperatures of PLA thermoplastic that induce damage. Thus, an essential requisite when designing a bioink would be cell support and protection during and after this procedure. When cell viability was examined by live/dead staining, it was found to retain greater than 85% of cell viability with no significant changes prior to and after printing (Fig. 4A and B). This suggested that such cell protection was partly associated with shear thinning behavior of bioink and the bioprinting system used, as previously reported [16].

This high cell viability was maintained in the cell-laden constructs and increased for long-term culture (Fig. 5A–F). Remarkably, predominant green fluorescence evidenced that chondrocytes were viable and well distributed into constructs over 1 month in vitro. These results also show morphology retention during their residence in it, which is very important for their functions. In addition, high cell viability was confirmed by proliferation assay data, which indicated cell growth over this period with a significant increase in PLA-HA-based bioink in comparison to control constructs

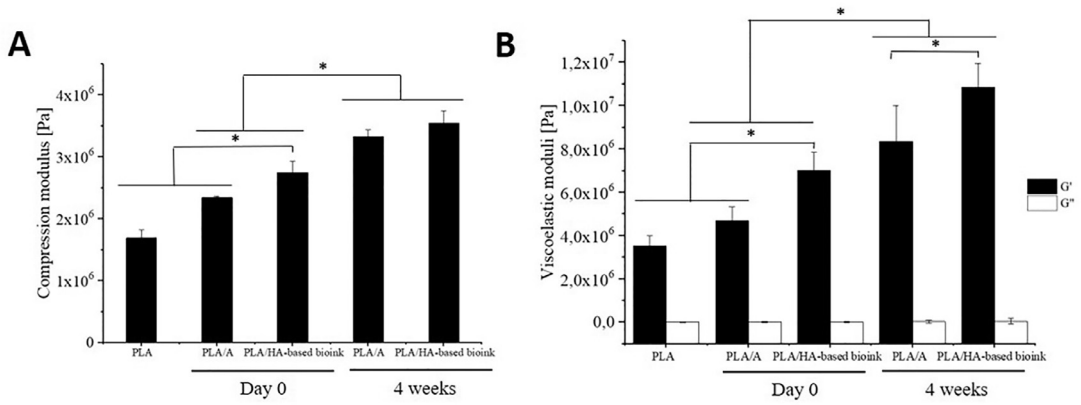

Fig. 3. Mechanical properties of bioprinted constructs. Compressive (a) and viscoelastic (b) modulus of PLA scaffold, hybrid scaffold of PLA-A bioink and PLA-HA-based bioink at day 0 and 28 days in culture. (mean ± SD, $n = 3$, Student's t-test, $^{*}p < 0.05$).

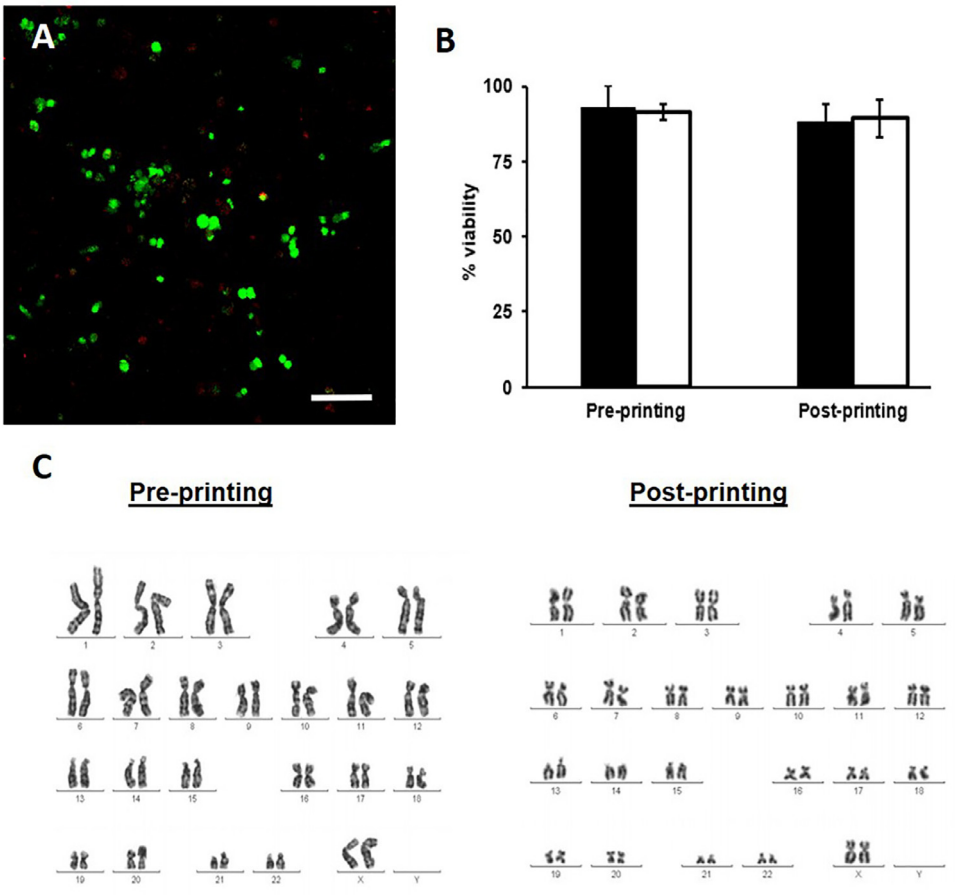

Fig. 4. Cell viability during bioprinting process. Live/Dead cell imaging analysis. (a) Representative image of bioprinted human chondrocytes in HA-based bioink, showing live (green) and dead (red) cells. (b) Percentage of chondrocyte viability in HA-based bioinks before and after the bioprinting process. (c) Karyotype of chondrocytes before and after bioprinting process.

with A ($p < 0.05$) (Fig. 5G). This evidenced the positive effect of HA on cell proliferation that has been reported in several studies [50–52].

3.4. Karyotype analysis

Cells were tested for genomic stability using a conventional analysis by G band techniques to assess whether the chondrocytes maintained their normal karyotype pre- and post-bioprinting. The karyotyping analysis of chondrocytes showed no karyotype changes before and after the bioprinting process obtaining a typical diploid karyotype (46, XX) (Fig. 4C). Cytogenetic karyotype analysis also revealed chromosomal stability, without any aberration related to the procedure.

3.5. Evaluation of neocartilage formation in hybrid bioprinted constructs

The ability to secrete a native ECM is another important issue to consider in this bioprinted construct as a substitute for cartilage

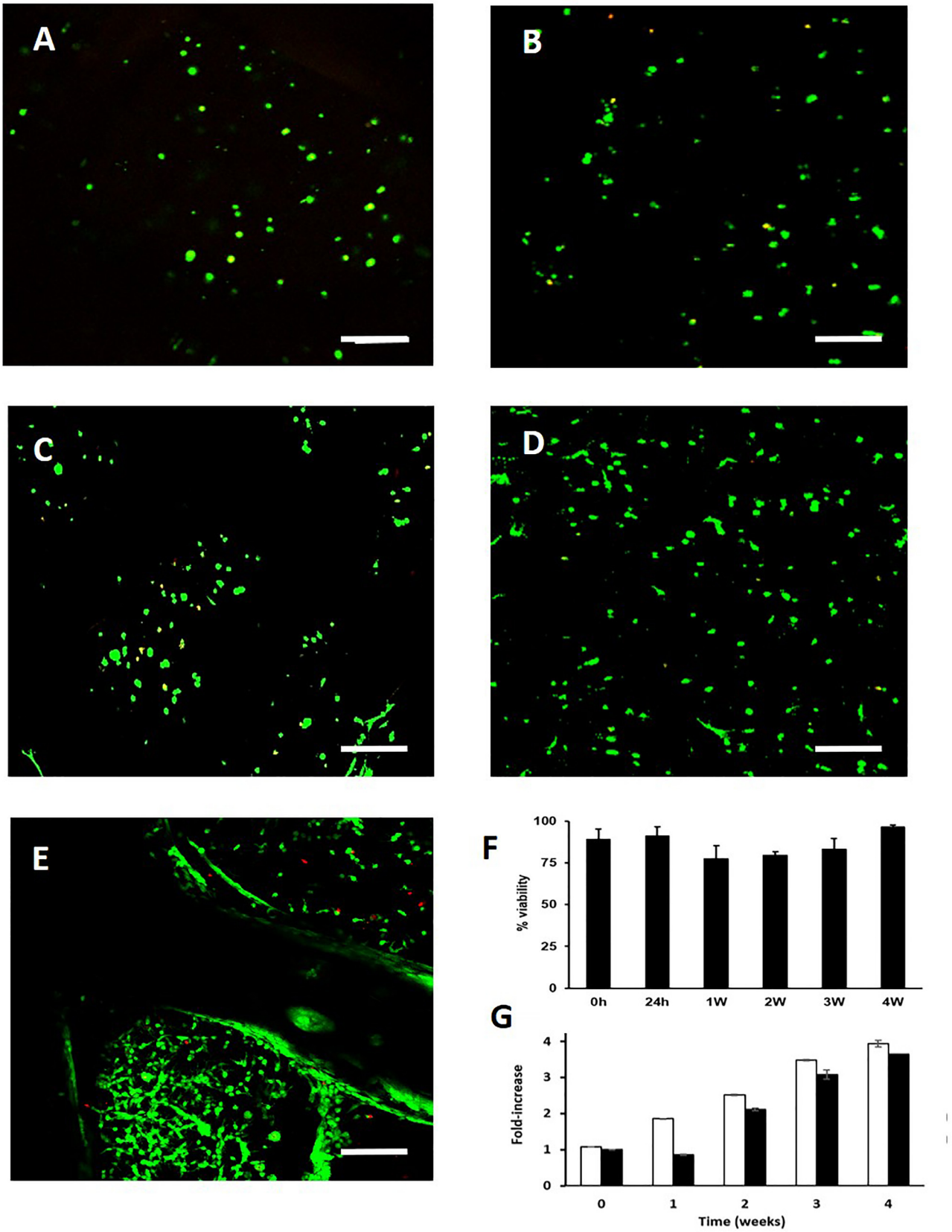

Fig. 5. Cell viability of chondrocytes in bioprinted construct with respect to time in culture. Representative image of bioprinted human chondrocytes in HA-based bioink after 24 h (a), 1 (b), 2 (c), 3 (d) and 4 weeks (e) in culture, showing live (green) and dead (red) cells. (f) Percentage of chondrocyte viability in HA-based bioinks with respect to time in culture. (g) Cell proliferation inside the HA-based (white) and alginate bioink (black). Error bars represent standard deviations ($n = 3$). Scale bar: 100 μm. (For interpretation of the references to colour in this figure legend, the reader is referred to the web version of this article.)

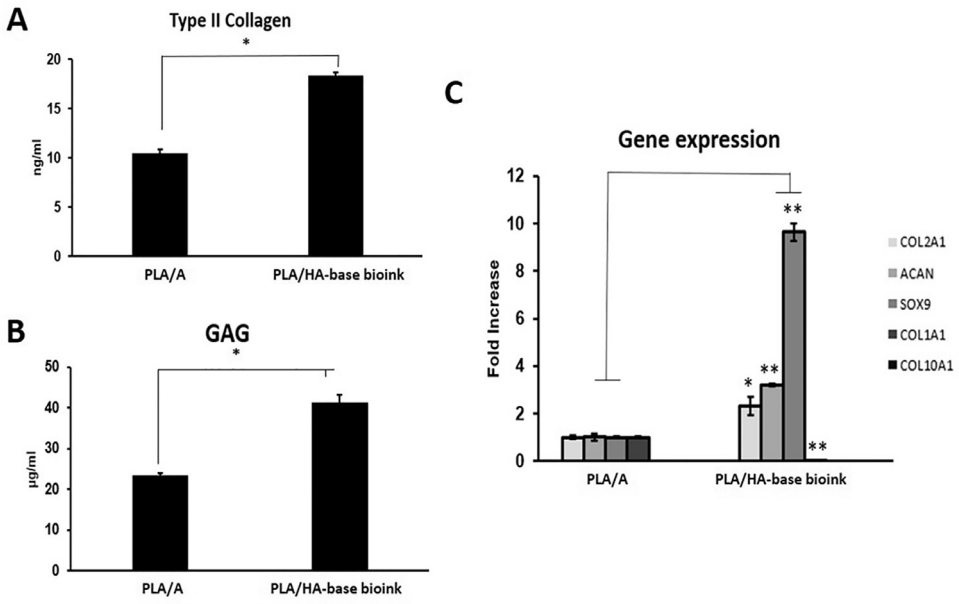

Fig. 6. Cartilage formation in hybrid 3D bioprinted constructs after 1 month in culture. Quantitative analysis of type II collagen (a) and GAG (b) in the total extract per scaffold (in 1 mL). (c) Gene expression levels of hyaline-specific chondrogenic marker genes (COL2A1, ACAN and SOX9), fibrotic maker (COL1A1) and hypertrophic marker (COL10A1) in bioprinted 3D hybrid construct (mean ± SD, $n = 3$, Student's t-test, $^{*}p < 0.05$, $^{**}p < 0.01$).

regeneration. The beneficial effect of HA on chondrogenic matrix production has been extensively reported in several studies [26,52–54], evidencing a stimulatory effect on synthesis of such matrix components, according to various mechanisms [3]. Fig. 6 shows the capacity of 3D bioprinted hybrid constructs to generate hyaline cartilage-specific ECM. The number of main components of this matrix such as type II collagen and GAG in hybrid PLA/HA-based bioink scaffolds after 4 weeks in culture was 18.32 ng and 41.37 µg, respectively. In both cases, values were significantly higher than controls with A (Fig. 6A and B).

HA regulation of chondrogenic phenotype was also analyzed by gene expression. In accordance with previous results, we observed an increased expression of hyaline cartilage-specific gene such as SOX9 in addition to COL2A1 and ACAN, while the expression of the fibrotic marker gene COL1A1 and the hypertrophic marker gene COL10A1 were low or undetectable when compared to control with A (Fig. 6C).

Taken together, these results suggest that bioprinted hybrid scaffold composed by PLA and HA-based bioink potentially supported AC formation in vitro as demonstrated by cartilage ECM deposition and chondrogenic gene expression.

4. Conclusions

In conclusion, we developed an HA-based bioink to produce highly viable and functional bioprinted 3D hybrid structures for AC regeneration. The mixture of HA with A provides the suitable mechanical properties to be used as cell-carrier biomaterial for construct fabrication by 3D bioprinting, that includes printability, gelling abilities, stiffness and good degradability. The application of this HA-based bioink to 3D bioprinting contributes to the creation of a proper biomimetic hybrid scaffold for AC regeneration, since it promotes chondrogenesis. In the future, we expect to investigate the cartilage regeneration in vivo, using such hybrid constructs in animal models, to achieve a possible clinical application.

Declaration of Competing Interest

None of the authors have a conflict of interest to declare.

Acknowledgements

The authors gratefully thank Ana Santos, Mohamed Tassi from the C.I.C. (University of Granada) and Purificacion Catalina from the Biobanco del Sistema Sanitario Público de Andalucia for the excellent technical assistance. This work was partially supported by MINECO MAT 2016-78778-R and PCIN-2015-051 projects (Spain), European Regional Development Fund (ERDF), by the Consejería de Economía, Conocimiento, Empresas y Universidad de la Junta de Andalucía and European Regional Development Fund (ERDF), ref. SOMM17/6109/UGR and by the Ministerio de Economía, Industria y Competitividad (FEDER funds, project RTC-2016-5451-1) (to JA.M and P.G-M). Additionally, it has been developed in the context of AdvanceCat with the support of ACCIÓ (Catalonia Trade & Investment; Generalitat de Catalunya) under the Catalonian European Regional Development Fund operational program, 2014-2020 (to P.G-M).

Supplementary materials

Supplementary material associated with this article can be found, in the online version, at doi:10.1016/j.actbio.2020.01.046.

References

[1] S.L. Francis, C. Di Bella, G.G. Wallace, P.F.M Choong, Cartilage tissue engineering using stem cells and bioprinting technology—barriers to clinical translation, Front. Surg. 5 (2018) 1–12, doi:10.3389/fsurg.2018.00070.
[2] F. You, B.F. Eames, X. Chen, Application of extrusion-based hydrogel bioprinting for cartilage tissue engineering, Int. J. Mol. Sci. 18 (2017) 8–14, doi:10.3390/ijms18071597.
[3] J. Yang, Y.S. Zhang, K. Yue, A. Khademhosseini, Cell-laden hydrogels for osteochondral and cartilage tissue engineering, Acta Biomater 57 (2017) 1–25, doi:10.1016/j.actbio.2017.01.036.

[4] A. Munaz, R.K. Vadivelu, J. St. John, M. Barton, H. Kamble, N.-T. Nguyen, Three-dimensional printing of biological matters, J. Sci. Adv. Mater. Devices. 1 (2016) 1–17, doi:10.1016/J.JSAMD.2016.04.001.
[5] Y. Wu, P. Kennedy, N. Bonazza, Y. Yu, A. Dhawan, I. Ozbolat, Three-Dimensional bioprinting of articular cartilage: a systematic review, Cartilage (2018), doi:10.1177/1947603518809410.
[6] Z. Izadifar, T. Chang, W. Kulyk, X. Chen, B.F. Eames, Analyzing biological performance of 3D-printed, cell-impregnated hybrid constructs for cartilage tissue engineering, Tissue Eng. - Part C Methods 22 (2016) 173–188, doi:10.1089/ten.tec.2015.0307.
[7] X. Ren, F. Wang, C. Chen, X. Gong, L. Yin, L. Yang, Engineering zonal cartilage through bioprinting collagen type II hydrogel constructs with biomimetic chondrocyte density gradient, BMC Musculoskelet. Disord 17 (2016) 1–10, doi:10.1186/s12891-016-1130-8.
[8] V.H.M. Mouser, R. Levato, A. Mensinga, W.J.A. Dhert, D. Gawlitta, J. Malda, Bioink development for three-dimensional bioprinting of hetero-cellular cartilage constructs, Connect. Tissue Res. 00 (2018) 1–15, doi:10.1080/03008207.2018.1553960.
[9] A.C. Daly, S.E. Critchley, E.M. Rencsok, D.J. Kelly, A comparison of different bioinks for 3D bioprinting of fibrocartilage and hyaline cartilage, Biofabrication 8 (2016) 1–10, doi:10.1088/1758-5090/8/4/045002.
[10] A. Abbadessa, V.H.M. Mouser, M.M. Blokzijl, D. Gawlitta, W.J.A. Dhert, W.E. Hennink, J. Malda, T. Vermonden, A synthetic thermosensitive hydrogel for cartilage bioprinting and its biofunctionalization with polysaccharides, Biomacromolecules 17 (2016) 2137–2147, doi:10.1021/acs.biomac.6b00366.
[11] K. Markstedt, A. Mantas, I. Tournier, H. Martínez Ávila, D. Hägg, P. Gatenholm, 3D bioprinting human chondrocytes with nanocellulose-alginate bioink for cartilage tissue engineering applications, Biomacromolecules 16 (2015) 1489–1496, doi:10.1021/acs.biomac.5b00188.
[12] S. Abdulghani, P.G. Morouço, Biofabrication for osteochondral tissue regeneration: bioink printability requirements, J. Mater. Sci. Mater. Med (2019) 30, doi:10.1007/s10856-019-6218-x.
[13] U. Jammalamadaka, K. Tappa, Recent advances in biomaterials for 3D printing and tissue engineering, J. Funct. Biomater (2018) 9, doi:10.3390/jfb9010022.
[14] J. Kundu, J.-.H. Shim, J. Jang, S.-.W. Kim, D.-.W. Cho, An additive manufacturing-based PCL-alginate-chondrocyte bioprinted scaffold for cartilage tissue engineering, J. Tissue Eng. Regen. Med. 9 (2015) 1286–1297, doi:10.1002/term.1682.
[15] B. Holmes, W. Zhu, J. Li, J.D. Lee, L.G. Zhang, Development of novel three-dimensional printed scaffolds for osteochondral regeneration, Tissue Eng. - Part A. 21 (2015) 403–415, doi:10.1089/ten.tea.2014.0138.
[16] J.M. Baena, G. Jiménez, E. López-Ruiz, C. Antich, C. Griñán-Lisón, M. Perán, P. Gálvez-Martín, J.A. Marchal, Volume-by-volume bioprinting of chondrocytes-alginate bioinks in high temperature thermoplastic scaffolds for cartilage regeneration, Exp. Biol. Med. (Maywood) 244 (2019) 13–21, doi:10.1177/1535370218821128.
[17] K. Hölzl, S. Lin, L. Tytgat, S. Van Vlierberghe, L. Gu, A. Ovsianikov, Bioink properties before, during and after 3D bioprinting, Biofabrication (2016) 8, doi:10.1088/1758-5090/8/3/032002.
[18] J.H. Shim, K.M. Jang, S.K. Hahn, J.Y. Park, H. Jung, K. Oh, K.M. Park, J. Yeom, S.H. Park, S.W. Kim, J.H. Wang, K. Kim, D.W. Cho, Three-dimensional bioprinting of multilayered constructs containing human mesenchymal stromal cells for osteochondral tissue regeneration in the rabbit knee joint, Biofabrication 8 (2016) 14102, doi:10.1088/1758-5090/8/1/014102.
[19] C.B. Knudson, Hyaluronan and CD44: strategic players for cell-matrix interactions during chondrogenesis and matrix assembly, Birth Defects Res. Part C - Embryo Today Rev 69 (2003) 174–196, doi:10.1002/bdrc.10013.
[20] I.T. Ozbolat, M. Hospodiuk, Current advances and future perspectives in extrusion-based bioprinting, Biomaterials 76 (2016) 321–343, doi:10.1016/j.biomaterials.2015.10.076.
[21] M. Kesti, M. Müller, J. Becher, M. Schnabelrauch, M. D'Este, D. Eglin, M. Zenobi-Wong, A versatile bioink for three-dimensional printing of cellular scaffolds based on thermally and photo-triggered tandem gelation, Acta Biomater. 11 (2015) 162–172, doi:10.1016/j.actbio.2014.09.033.
[22] M.T. Poldervaart, B. Goversen, M. De Ruijter, A. Abbadessa, F.P.W. Melchels, F.C. Öner, W.J.A. Dhert, T. Vermonden, J. Alblas, 3D bioprinting of methacrylated hyaluronic acid (MeHA) hydrogel with intrinsic osteogenicity, PLoS ONE (2017) 12, doi:10.1371/journal.pone.0177628.
[23] D. Petta, A.R. Armiento, D. Grijpma, M. Alini, D. Eglin, M. D'Este, 3D bioprinting of a hyaluronan bioink through enzymatic-and visible light-crosslinking, Biofabrication 10 (2018) 044104, doi:10.1088/1758-5090/aadf58.
[24] S. Sakai, K. Mochizuki, Y. Qu, M. Mail, M. Nakahata, M. Taya, Peroxidase-catalyzed microextrusion bioprinting of cell-laden hydrogel constructs in vaporized ppm-level hydrogen peroxide, Biofabrication (2018) 10, doi:10.1088/1758-5090/aadc9e.
[25] E.A. Kiyotake, A.W. Douglas, E.E. Thomas, S.L. Nimmo, M.S. Detamore, Development and quantitative characterization of the precursor rheology of hyaluronic acid hydrogels for bioprinting, Acta Biomater. 95 (2019) 176–187, doi:10.1016/j.actbio.2019.01.041.
[26] A.C. Daly, S.E. Critchley, E.M. Rencsok, I.A.D. Mancini, V.H.M. Mouser, A. Abbadessa, R. Levato, W.E. Hennink, T. Vermonden, D. Gawlitta, J. Malda, Development of a thermosensitive HAMA- containing bio-ink for the fabrication of composite cartilage repair constructs fixation of hydrogel constructs for cartilage repair in the equine model: a challenging issue fixation of hydrogel constructs for cartil, Biofabrication (2017) 9 https://doi.org/, doi:10.1088/1758-5090/aa6265.
[27] A. Mazzocchi, M. Devarasetty, R. Huntwork, S. Soker, A. Skardal, Optimization of collagen type I-hyaluronan hybrid bioink for 3D bioprinted liver microenvironments, Biofabrication 11 (2018) 015003, doi:10.1088/1758-5090/aae543.
[28] T.Y. Park, Y.J. Yang, D.-H. Ha, D.-W. Cho, H.J. Cha, Marine-derived natural polymer-based bioprinting ink for biocompatible, durable, and controllable 3D constructs., Biofabrication 11 (2019) 035001, doi:10.1088/1758-5090/ab0c6f.
[29] N. Law, B. Doney, H. Glover, Y. Qin, Z.M. Aman, T.B. Sercombe, L.J. Liew, R.J. Dilley, B.J. Doyle, Characterisation of hyaluronic acid methylcellulose hydrogels for 3D bioprinting, J. Mech. Behav. Biomed. Mater. 77 (2018) 389–399, doi:10.1016/j.jmbbm.2017.09.031.
[30] S. Khalil, W. Sun, Bioprinting endothelial cells with alginate for 3D tissue constructs, J. Biomech. Eng (2009) 131, doi:10.1115/1.3128729.
[31] J. Park, S.J. Lee, S. Chung, J.H. Lee, W.D. Kim, J.Y. Lee, S.A. Park, Cell-laden 3D bioprinting hydrogel matrix depending on different compositions for soft tissue engineering: characterization and evaluation, Mater. Sci. Eng. C. Mater. Biol. Appl. 71 (2017) 678–684, doi:10.1016/j.msec.2016.10.069.
[32] E. López-Ruiz, G. Jiménez, W. Kwiatkowski, E. Montañez, F. Arrebola, E. Carrillo, S. Choe, J.A. Marchal, M. Perán, Impact of TGF-β family-related growth factors on chondrogenic differentiation of adipose-derived stem cells isolated from lipoaspirates and infrapatellar fat pads of osteoarthritic patients, Eur. Cells Mater. 35 (2018) 209–224, doi:10.22203/eCM.v035a15.
[33] H. Park, H.J. Lee, H. An, K.Y. Lee, Alginate hydrogels modified with low molecular weight hyaluronate for cartilage regeneration, Carbohydr. Polym 162 (2017) 100–107, doi:10.1016/j.carbpol.2017.01.045.
[34] E. Amann, P. Wolff, E. Breel, M. van Griensven, E.R. Balmayor, Hyaluronic acid facilitates chondrogenesis and matrix deposition of human adipose derived mesenchymal stem cells and human chondrocytes co-cultures, Acta Biomater 52 (2017) 130–144, doi:10.1016/j.actbio.2017.01.064.
[35] K. Kawasaki, M. Ochi, Y. Uchio, N. Adachi, M. Matsusaki, Hyaluronic acid enhances proliferation and chondroitin sulfate synthesis in cultured chondrocytes embedded in collagen gels, J. Cell. Physiol. 179 (1999) 142–148, doi:10.1002/(SICI)1097-4652(199905)179:2⟨142::AID-JCP4⟩3.0.CO;2-Q.
[36] S. Marlovits, M. Hombauer, M. Truppe, V. Vècsei, W. Schlegel, Changes in the ratio of type-I and type-II collagen expression during monolayer culture of human chondrocytes, J. Bone Jt. Surg. - Ser. B. 86 (2004) 286–295, doi:10.1302/0301-620X.86B2.14918.
[37] T. Vinardell, E.J. Sheehy, C.T. Buckley, D.J. Kelly, Phenotypic stability of cartilaginous tissues engineered from different stem cell sources, Tissue Eng. Part A. 18 (2012) 1161–1170, doi:10.1089/ten.tea.2011.0544.
[38] J.A. Burdick, G.D. Prestwich, Hyaluronic acid hydrogels for biomedical applications, Adv. Mater. 23 (2011) H41–H56, doi:10.1002/adma.201003963.
[39] Z. Liu, M. Zhang, B. Bhandari, C. Yang, Impact of rheological properties of mashed potatoes on 3D printing, J. Food Eng. 220 (2018) 76–82, doi:10.1016/j.jfoodeng.2017.04.017.
[40] H. Park, H.J. Lee, H. An, K.Y. Lee, Alginate hydrogels modified with low molecular weight hyaluronate for cartilage regeneration, Carbohydr. Polym. 162 (2017) 100–107, doi:10.1016/j.carbpol.2017.01.045.
[41] I.E. Erickson, A.H. Huang, S. Sengupta, S. Kestle, J.A. Burdick, R.L. Mauck, Macromer density influences mesenchymal stem cell chondrogenesis and maturation in photocrosslinked hyaluronic acid hydrogels, Osteoarthr. Cartil. 17 (2009) 1639–1648, doi:10.1016/j.joca.2009.07.003.
[42] I.E. Erickson, S.R. Kestle, K.H. Zellars, M.J. Farrell, M. Kim, J.A. Burdick, R.L. Mauck, High mesenchymal stem cell seeding densities in hyaluronic acid hydrogels produce engineered cartilage with native tissue properties, Acta Biomater. 8 (2012) 3027–3034, doi:10.1016/j.actbio.2012.04.033.
[43] E. Amann, P. Wolff, E. Breel, M. van Griensven, E.R. Balmayor, Hyaluronic acid facilitates chondrogenesis and matrix deposition of human adipose derived mesenchymal stem cells and human chondrocytes co-cultures, Acta Biomater 52 (2017) 130–144, doi:10.1016/j.actbio.2017.01.064.
[44] T. Franz, E.M. Hasler, R. Hagg, C. Weiler, R.P. Jakob, P. Mainil-Varlet, In situ compressive stiffness, biochemical composition, and structural integrity of articular cartilage of the human knee joint., Osteoarthr. Cartil. 9 (2001) 582–592, doi:10.1053/joca.2001.0418.
[45] D.H. Rosenzweig, E. Carelli, T. Steffen, P. Jarzem, L. Haglund, 3D-Printed ABS and PLA scaffolds for cartilage and nucleus pulposus tissue regeneration, Int. J. Mol. Sci. 16 (2015) 15118–15135, doi:10.3390/ijms160715118.
[46] L. Moroni, J.R. de Wijn, C.A. van Blitterswijk, 3D fiber-deposited scaffolds for tissue engineering: influence of pores geometry and architecture on dynamic mechanical properties, Biomaterials 27 (2006) 974–985, doi:10.1016/j.biomaterials.2005.07.023.
[47] Y. Xu, X. Guo, S. Yang, L. Li, P. Zhang, W. Sun, C. Liu, S. Mi, Construction of bionic tissue engineering cartilage scaffold based on three-dimensional printing and oriented frozen technology, J. Biomed. Mater. Res. A. 106 (2018) 1664–1676, doi:10.1002/jbm.a.36368.
[48] W. Schuurman, V. Khristov, M.W. Pot, P.R. van Weeren, W.J.A. Dhert, J. Malda, Bioprinting of hybrid tissue constructs with tailorable mechanical properties, Biofabrication 3 (2011) 021001, doi:10.1088/1758-5082/3/2/021001.
[49] Z. Izadifar, X. Chen, W. Kulyk, Strategic design and fabrication of engineered scaffolds for articular cartilage repair, J. Funct. Biomater. 3 (2012) 799–838, doi:10.3390/jfb3040799.
[50] M. Abe, M. Takahashi, A. Nagano, The effect of hyaluronic acid with different molecular weights on collagen crosslink synthesis in cultured chondrocytes embedded in collagen gels, J. Biomed. Mater. Res. A. 75 (2005) 494–499, doi:10.1002/jbm.a.30452.
[51] K. Kawasaki, M. Ochi, Y. Uchio, N. Adachi, M. Matsusaki, Hyaluronic acid enhances proliferation and chondroitin sulfate synthesis in cultured chondrocytes

embedded in collagen gels, J. Cell. Physiol 179 (1999) 142–148, doi:10.1002/(SICI)1097-4652(199905)179:2⟨142::AID-JCP4⟩3.0.CO;2-Q.
[52] C. Chung, J. Mesa, M.A. Randolph, M. Yaremchuk, J.A. Burdick, Influence of gel properties on neocartilage formation by auricular chondrocytes photoencapsulated in hyaluronic acid networks, J. Biomed. Mater. Res. - Part A. 77 (2006) 518–525, doi:10.1002/jbm.a.30660.
[53] H. Park, K.Y. Lee, Cartilage regeneration using biodegradable oxidized alginate/hyaluronate hydrogels, J. Biomed. Mater. Res. Part A. (2014) n/a-n/a, doi:10.1002/jbm.a.35126.
[54] M. Akmal, The effects of hyaluronic acid on articular chondrocytes, J. Bone Jt. Surg. - Br. 87–B (2005) 1143–1149, doi:10.1302/0301-620X.87B8.15083.